Supplementary Information (SI) for Journal of Materials Chemistry C.
This journal is © The Royal Society of Chemistry

Supporting Information

Effect of molecular architecture on the self-assembly and photophysical properties of naphthalene imide-benzimidazole derivatives and their application in solution-processable OLEDs

Nandan Kumar,[a] Anil Kumar,[b] Paresh Kumar Behera,[a] Dharmendra Adak,[a] Alakananda Patra,[c] Sandeep Kumar,[d] Shiang-Yi Lee,[b] Jwo-Huei Jou*[b,] and Ammathnadu Sudhakar Achalkumar*[a,e]

[a]*Department of Chemistry, Indian Institute of Technology Guwahati, Guwahati, 781039, Assam, India.*
[b]*Department of Materials Science and Engineering, National Tsing Hua University, No. 101, Section 2, Guangfu Rd., East District, Hsinchu, Taiwan, 30013*

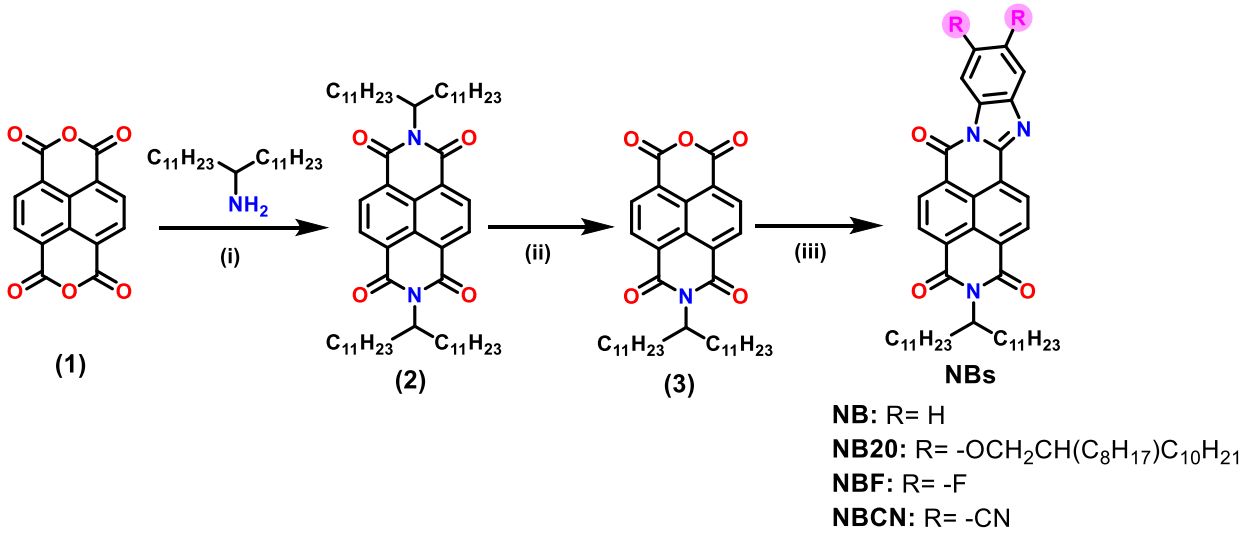
[c]*Raman Research Institute, Bengaluru, C. V. Raman Avenue, 5th Cross Road, Sadashivanagar, Near Mekhri Circle, Bengaluru, Karnataka 560080.*
[d] *Department of Chemistry and Biochemistry, Sharda School of Engineering & Science, Sharda University, Greater Noida, India*
[e] *School of Interdisciplinary Studies and Sustainability, Indian Institute of Technology Guwahati, Guwahati, 781039, Assam, India.*

Serial Number	Contents	Page numbers
1	Materials and methods	S2
2	Experimental Section	S3-S5
3	NMR Spectra	S6-S11
4	MALDI-TOF Mass spectra	S12-S14
5	Polarizing Optical Microscopy	S15
6	Differential scanning calorimetry	S16
7	X-ray diffraction studies	S16-S17
8	Photophysical properties	S18-S19
9	Time resolved photoluminescence studies	S19
10	Electrochemical properties	S20
11	DFT Studies	S21-S25
12	OLED device fabrication and measurement	S26
13	References	S26-S27

1. Materials and methods Commercially available chemicals were used without any purification; solvents were dried following the standard procedures. Chromatography was performed using either silica gel (60-120 mesh) or neutral aluminium oxide. For thin layer chromatography, aluminium sheets pre-coated with silica gel were employed. IR spectra were recorded on a Perkin Elmer IR spectrometer at normal temperature by using KBr pellet. The spectral positions are given in wave number (cm^{-1}) unit. NMR spectra were recorded using Bruker 600 MHz NMR spectrometer. For 1H NMR spectra, the chemical shifts are reported in ppm relative to TMS as an internal standard. Coupling constants are given in Hz. Mass spectra were determined from MALDI-TOF mass spectrometer using α-Cyano-4-hydroxycinnamic acid as a matrix or high resolution Mass Spectrometer. The mesogenic compounds were investigated for their liquid crystalline behaviour (birefringence and fluidity) by employing a polarizing optical microscope (Nikon Eclipse LV100POL) equipped with a programmable hot stage (Mettler Toledo FP90). Clean glass slides and coverslips were employed for the polarizing optical microscopic observations. The transition temperatures and associated enthalpy changes were determined by differential scanning calorimeter (Mettler Toledo DSC1) under nitrogen atmosphere. Peak temperatures obtained in DSC corresponding to transitions were in agreement with the polarizing optical microscopic observations. The transition temperatures obtained from calorimetric measurements of the first heating and cooling cycles at a rate of 5 °C/min are tabulated. Variable temperature X-ray diffraction measurements were carried out with samples filled in Lindemann capillaries. The apparatus essentially involved a high resolution X-ray powder diffractometer (PANalytical X'pert pro) with a high resolution fast detector PIXCEL. The temperature of the sample was varied using a Mettler hot stage/ programmer (FP82HT/FP90). Thermogravimetric analysis (TGA) was performed using thermogravimetric analyzer (Mettler Toledo, model TG/SDTA 851 e) under a nitrogen flow at a heating rate of 10 °C/min. UV-Vis spectra were obtained by using Perkin-Elmer Lambda 750, UV/VIS/NIR spectrometer. Fluorescence emission spectra in solution state were recorded with Horiba Fluoromax-4 fluorescence spectrophotometer or Perkin Elmer LS 50B spectrometer. Cyclic Voltammetry studies were carried out using a Versa Stat 3 (Princeton Applied Research) Electrochemical workstation.

2. Experimental Section

2.1 Synthetic Scheme



Reagent and Conditions; (i) Imidazole, $Zn(OAc)_2$,165 °C, microwave, 45 min, 76 %; (ii) KOH, t-BuOH, 100 °C, 1h, 49 %; (iii) 1,2-diaminobenzene, acetic acid, 100 °C, 12 h.

Step 1: Synthesis and characterization of compound (2)[1,2]:

Naphthalene-3,4,9,10-tetracarboxylic dianhydride (1 eq.), swallowtail amine (2.2 eq.)[5], zinc acetate (2 eq.) and imidazole (1 g) were taken in a microwave vessel, flushed with nitrogen and put in microwave reactor. The mixture was heated at 165 °C for 35 minutes at 35 W and 100 psi pressure. After cooling, reaction mixture was poured in 2(N) HCl (10 mL) and extracted with chloroform. Organic mixture was washed with water and saturated sodium chloride solution. The crude compound was purified by silica gel column chromatography using 40% chloroform-hexane system. Further purification was done by recrystallization from chloroform-methanol system. R_f = 0.6 (50% Chloroform-Hexane); White solid, Yield: 76%; IR ν_{max} in cm^{-1}: 2917, 2850, 1712, 1665, 1577, 1469, 1455, 1393, 1323, 1250, 1209, 1194, 1151, 1089, 988, 965, 879, 858, 771, 717; ^{1}H NMR (400 MHz, $CDCl_3$, 299 K): 8.02 (bs, 4H, H_{Ar}), 5.18-5.12 (m, 2H, 2 × -CH), 2.24-2.19 (m, 4H, 2 × $-CH_2$), 1.84-1.82 (m, 4H, 2 × $-CH_2$), 1.26-1.19 (m, 72H, 36 × $-CH_2$), 0.87-0.84 (t, J = 6.8 Hz, 12H, 4 × $-CH_3$); ^{13}C NMR (100 MHz, $CDCl_3$, 298.1 K): δ 162.46, 130.80, 127.92, 127.22, 126.16, 55.36, 32.25, 31.88, 29.57, 29.53, 29.48, 29.45, 29.30, 26.89, 22.66, 14.09; MALDI-TOF mass calculated for $C_{60}H_{98}N_2O_4$ ($M+H^+$) : 911.7507, found: 911.7502.

Step 2: Synthesis and characterization of compound (3)[3]:

Compound 2 (1 eq.) was taken in a round bottom flask with KOH (1 eq.) in tert-butanol (20 mL). The resulting mixture was refluxed for 55 minutes. The hot basic mixture was then poured into 17 mL of acetic acid and 7 mL of HCl. After the mixture cools it was taken in chloroform. The organic layer was washed with water three times (3 x 30 mL) followed by brine. The organic layer was concentrated and chromatographed on a silica gel column using chloroform as eluent to get the pure product as white solid. Yield: 49%; R_f = 0.4 (2% Methanol-chloroform); IR ν_{max} in cm^{-1} : 2920, 2851, 1702, 1660, 1628, 1586, 1540, 1465, 1376, 1339, 1217, 1105, 952, 872, 833, 777,

721; ^{1}H NMR (400 MHz, $CDCl_3$, 299 K): 8.77 (s, 2H, H_{Ar}), 8.76 (s, 2H, H_{Ar}), 5.17-5.13 (m, 1H, -CH), 2.23-2.17 (m, 2H, -CH_2), 1.86-1.84 (m, 2H, -CH_2), 1.29-1.19 (m, 36H, 18 × -CH_2), 0.87-0.84 (t, J = 6.8 Hz, 6H, 2 × -CH_3); ^{13}C NMR (100 MHz, $CDCl_3$, 298.1 K): δ 164.16, 162.98, 131.34, 130.61, 127.05, 126.81, 126.30, 55.17, 32.30, 31.90, 29.60, 29.58, 29.55, 29.51, 29.48, 29.31, 26.90, 22.67, 14.10; MALDI-TOF mass calculated for $C_{37}H_{51}NO_5$ ($M+H^+$) : 590.3767, found: 590.3804.

Step 3: Procedure for synthesis of NBs[4]

A mixture of compound 3 (1 eq.), diamine (1.1 eq.) and acetic acid (20 mL) were heated at 100 °C for 12 h. After cooling to room temperature, the reaction mixture was extracted with chloroform. The organic layer was washed with water and saturated sodium chloride solution, dried over Na_2SO_4, and concentrated. The crude product was purified by silica gel column chromatography using 20% chloroform-hexane system.

NB: R_f = 0.5 (40% Chloroform-Hexane); Green powdered solid, Yield: 62%; IR ν_{max} in cm^{-1}: 2920, 2851, 1694, 1657, 1615, 1579, 1546, 1509, 1463, 1445, 1394, 1374, 1335, 1305, 1240, 1167, 1111, 1011, 982, 867, 759, 741, 722; ^{1}H NMR (400 MHz, $CDCl_3$, 299 K): 8.93-8.88 (m, 2H, H_{Ar}), 8.76 (bs, 2H, H_{Ar}), 8.50-8.49 (m, 1H, H_{Ar}), 7.90-7.88 (d, J = 7.2 Hz, 1H, H_{Ar}), 7.54-7.49 (m, 2H, H_{Ar}), 5.20-5.15 (m, 1H, -CH), 2.27-2.18 (m, 2H, -CH_2), 1.89-1.86 (m, 2H, -CH_2), 1.26-1.20 (m, 36H, 16 × -CH_2), 0.86-0.83 (t, J = 7.2 Hz, 6H, 2 × -CH_3); ^{13}C NMR (100 MHz, $CDCl_3$, 298.1 K): δ 159.13, 159.11, 147.66, 147.64, 143.81,143.79, 131.85, 131.83, 131.08, 127.49, 126.87, 126.54, 126.44, 125.61, 125.59, 120.75, 115.84, 55.21, 32.36, 31.90, 29.61, 29.60, 29.58, 29.54, 29.32, 26.97, 22.66, 14.09; MALDI-TOF mass calculated for $C_{43}H_{55}N_3O_3$ (M^+) : 661.4243, found: 661.4199.

NB20: R_f = 0.6 (40% Chloroform-Hexane); Purple solid, Yield: 73%; IR ν_{max} in cm^{-1}: 2920, 2851, 1698, 1659, 1616, 1599, 1578, 1542, 1483, 1456, 1406, 1378, 1332, 1288, 1240, 1214, 1170, 1146, 1098, 847, 826, 766, 757, 721; ^{1}H NMR (400 MHz, $CDCl_3$, 299 K): 8.83-8.81 (d, J = 7.6 Hz, 1H, H_{Ar}), 8.78-8.76 (d, J = 7.6 Hz, 1H, H_{Ar}), 8.73 (bs, 2H, H_{Ar}), 7.96 (s, 1H, H_{Ar}), 7.32 (s, 1H, H_{Ar}), 5.17 (m, 1H, -CH), 4.04-4.03 (d, J = 4.8 Hz, 2H, -OCH_2), 3.98-3.97 (d, J = 4.8 Hz, 2H, -OCH_2), 2.24 (bs, 2H, -CH_2), 1.89 (bs, 4H, 2 ×-CH_2), 1.55 (bs, 4H, 2 ×-CH_2), 1.27-1.20 (m, 96H, 48 × -CH_2), 0.88-0.85 (m, 18H, 6 × -CH_3); ^{13}C NMR (100 MHz, $CDCl_3$, 298.1 K): δ 159.44, 150.60, 149.67, 146.03, 141.52, 137.80, 130.71, 129.47, 127.66, 127.30, 126.11, 125.33, 120.35, 103.76, 99.30, 72.15, 55.06, 38.16, 38.10, 31.95, 29.71, 29.60, 29.52, 29.41, 22.71, 22.67, 14.13, 14.10; MALDI-TOF mass calculated for $C_{83}H_{135}N_3O_5$ ($M+H^+$) : 1255.0402, found: 1255.362.

NBF: R_f = 0.4 (40% Chloroform-Hexane); Green powdered solid, Yield: 50%; IR ν_{max} in cm^{-1} :3111, 2956, 2920, 2852, 1700, 1665, 1618, 1603, 1579, 1552, 1478, 144, 1378, 1339, 1293, 1243, 1217, 1147, 1125, 1092, 857, 766, 757, 721; ^{1}H NMR (400 MHz, $CDCl_3$, 299 K): 8.90-8.87 (t, J = 6.0 Hz, 2H, H_{Ar}), 8.78 (bs, 2H, H_{Ar}), 8.33-8.30 (t, J = 6.6 Hz, 1H, H_{Ar}), 7.65-7.62 (t, J = 6.6 Hz, 1H, H_{Ar}), 5.18-5.16 (m, 1H, -CH), 2.25-2.18 (m, 2H, -CH_2), 1.87-1.86 (m, 2H, -CH_2), 1.59-1.57 (m, 2H, -CH_2), 1.25-1.19 (m, 34H, 17 ×-CH_2), 0.86-0.83 (t, J = 6.0 Hz, 6H, 2 × -CH_3); ^{13}C NMR (100 MHz, $CDCl_3$, 298.1 K): δ 158.97, 149.01, 139.55, 131.53, 127.55, 127.37, 126.79, 126.43, 125.58, 124.65, 108.48, 108.32, 104.60, 104.40, 55.31, 32.31, 31.89, 29.59, 29.56, 29.51, 29.49,

29.31, 26.93, 22.65, 14.08; MALDI-TOF mass calculated for $C_{43}H_{53}F_2N_3O_3$ (M^+) : 697.4055, found: 697.4101.

NBCN: R_f = 0.4 (40% Chloroform-Hexane); Green powdered solid, Yield: 39%; IR ν_{max} in cm^{-1} :3101, 2920, 2852, 2232, 1703, 1669, 1616, 1602, 1579, 1544, 1508, 1461, 1410, 1335, 1308, 1243, 1171, 1092, 1073, 984, 911, 898, 878, 768, 758, 720; ^{1}H NMR (600 MHz, $CDCl_3$, 299 K): 9.09-9.07 (d, *J* = 7.8 Hz, 1H, H_{Ar}), 9.04-9.02 (m, 2H, H_{Ar}), 8.89 (bs, 2H, H_{Ar}), 8.34 (s, 1H, H_{Ar}), 5.18-5.16 (m, 1H, -CH), 2.24-2.18 (m, 2H, -CH_2), 1.87 (m, 2H, -CH_2), 1.30-1.19 (m, 36H, 18 ×-CH_2), 0.85-0.83 (t, *J* = 7.2 Hz, 6H, 2 × -CH_3); ^{13}C NMR (150 MHz, $CDCl_3$, 298.1 K): δ 159.07, 152.44, 146.06, 133.96, 132.73, 128.85, 127.59, 126.60, 126.07, 125.69, 123.43, 121.86, 115.61, 115.46, 113.14, 112.27, 55.53, 32.26, 31.89, 29.59, 29.55, 29.50, 29.46, 29.32, 26.92, 22.67, 14.11; MALDI-TOF mass calculated for $C_{45}H_{53}N_5O_3$ (M^+) : 711.4148, found: 711.4101.

3. NMR Spectra

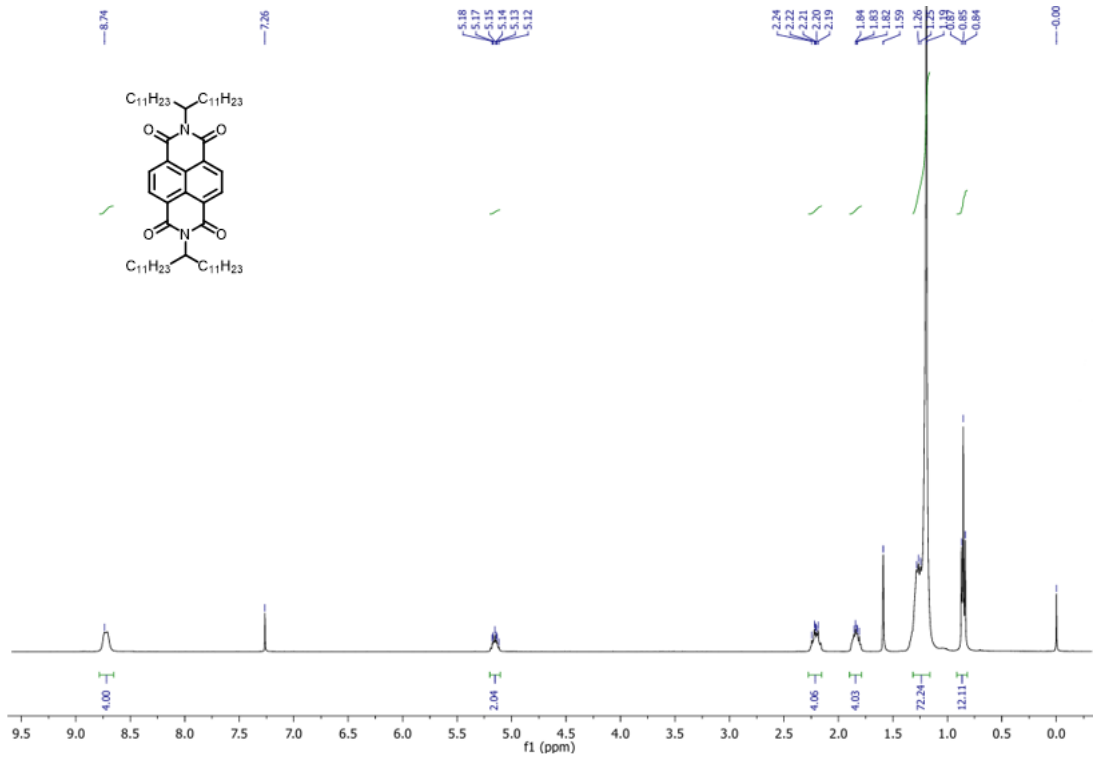


Figure S1. ^{1}H NMR (400 MHz) spectrum of compound **2** in $CDCl_3$.

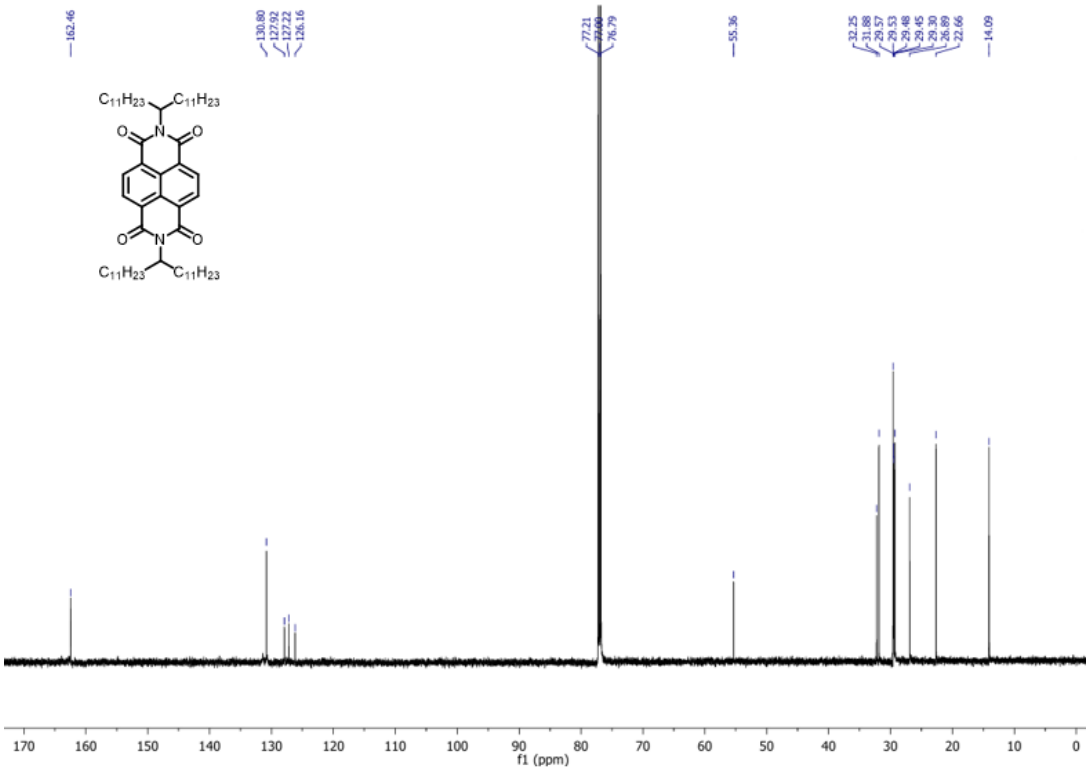


Figure S2. ^{13}C NMR (100 MHz) spectrum of compound **2** in $CDCl_3$.

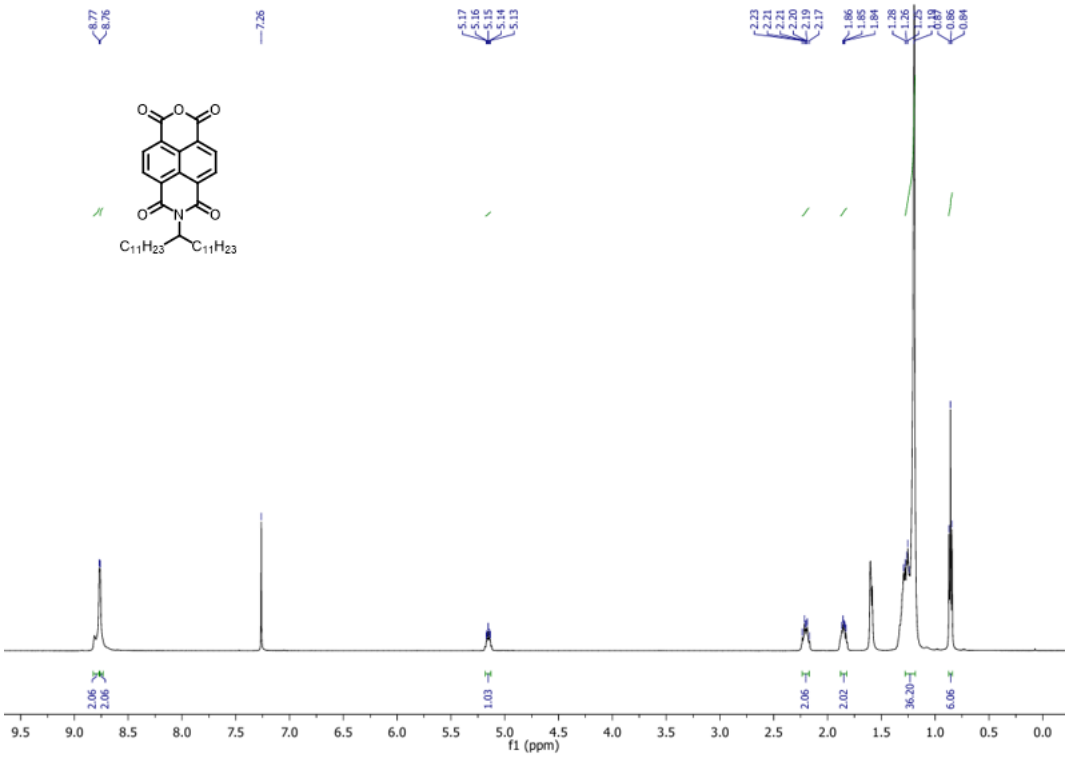


Figure S3. ^{1}H NMR (400 MHz) spectrum of compound **3** in $CDCl_3$.

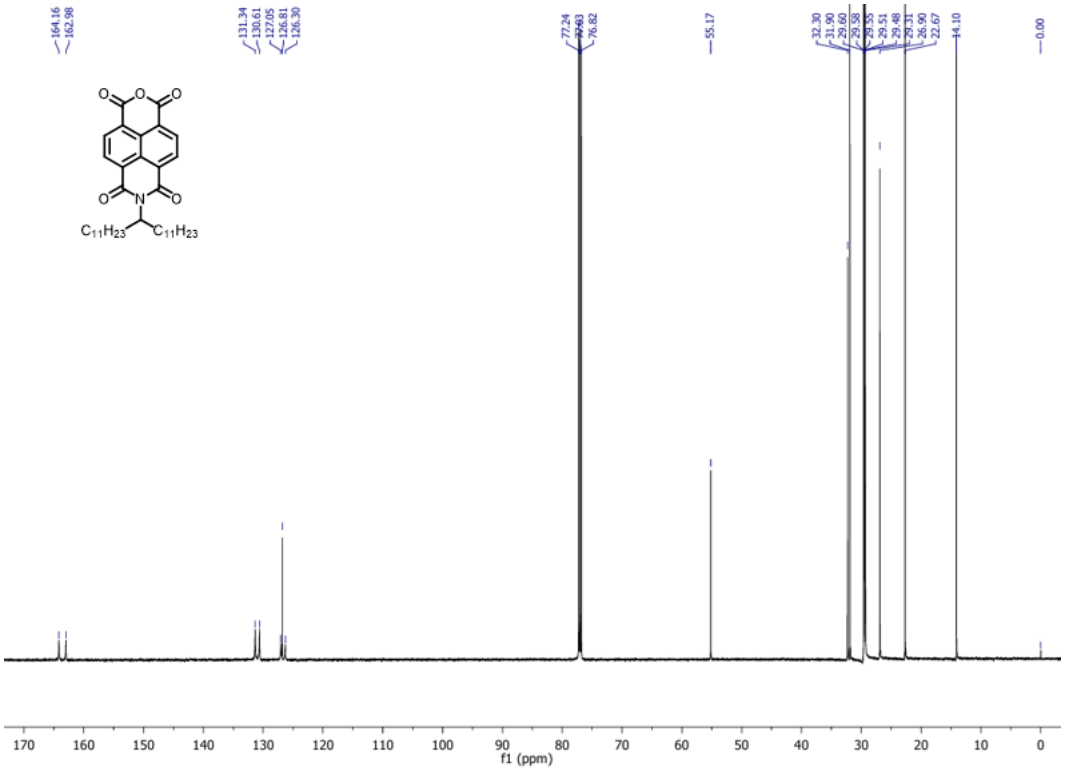


Figure S4. ^{13}C NMR (100 MHz) spectrum of compound **3** in $CDCl_3$.

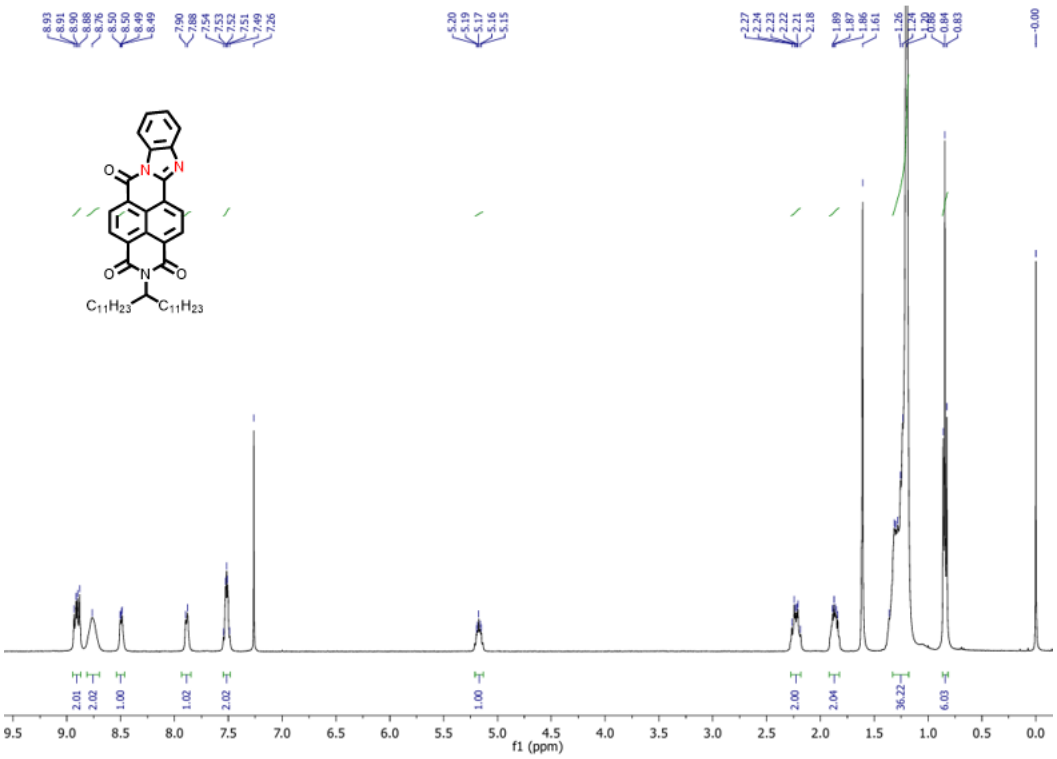


Figure S5. ^{1}H NMR (400 MHz) spectrum of **NB** in $CDCl_3$.

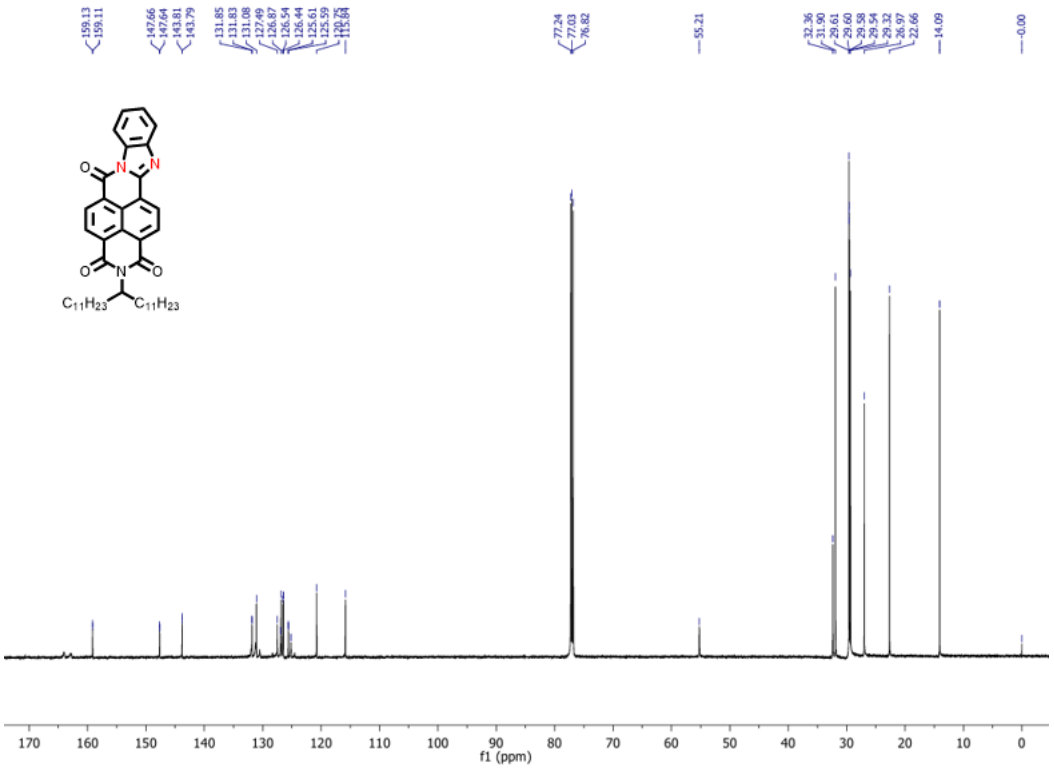


Figure S6. ^{13}C NMR (100 MHz) spectrum of **NB** in $CDCl_3$.

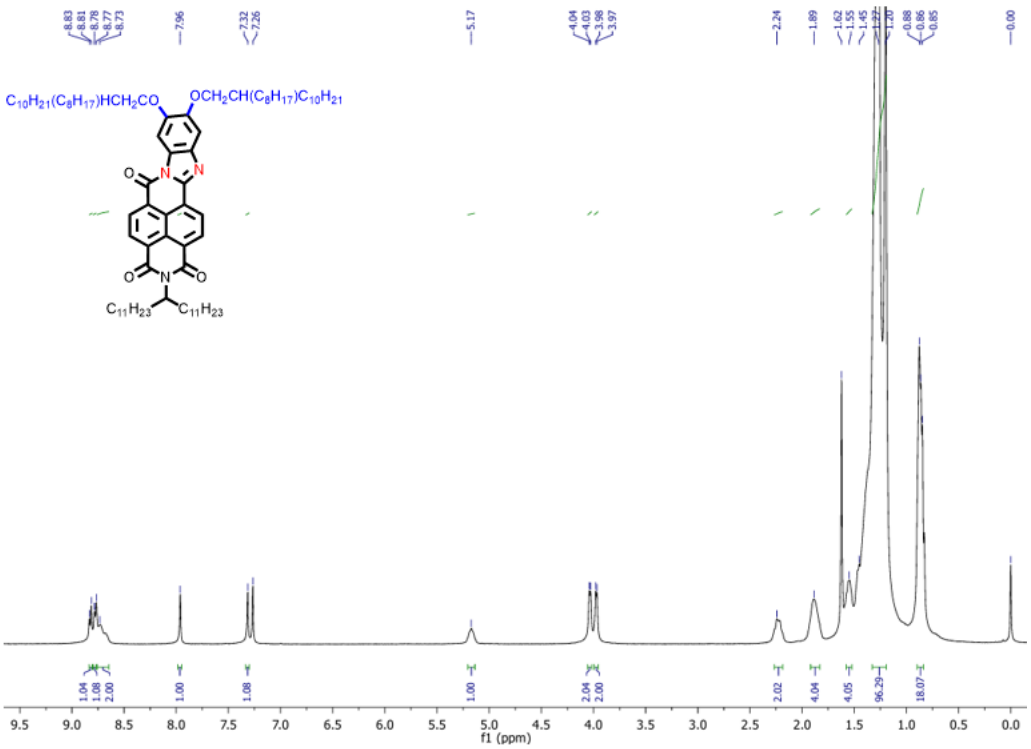


Figure S7. ^{1}H NMR (400 MHz) spectrum of **NB20** in $CDCl_3$.

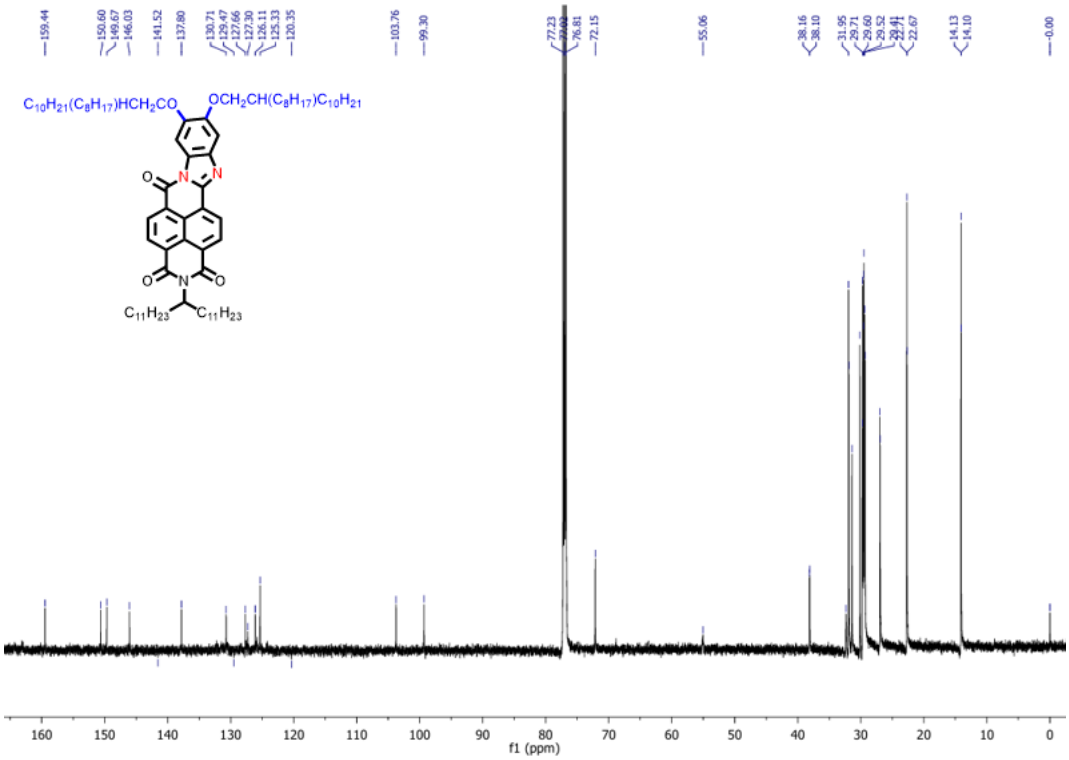


Figure S8. ^{13}C NMR (100 MHz) spectrum of **NB20** in $CDCl_3$.

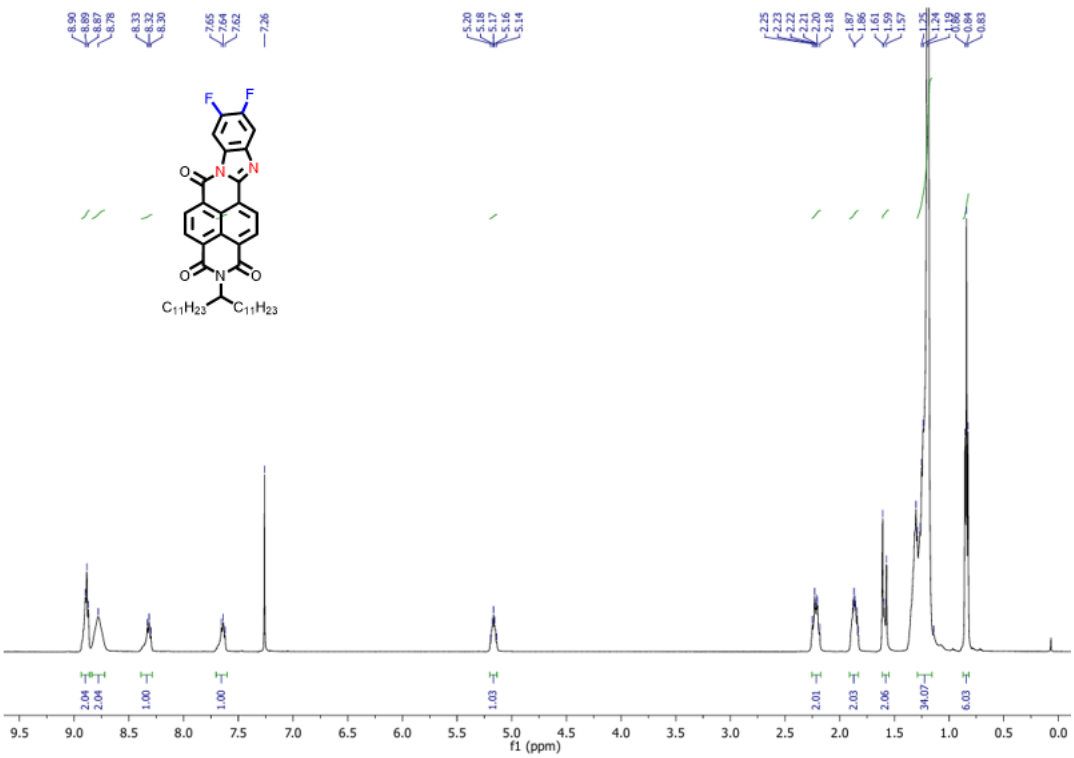


Figure S9. ^{1}H NMR (400 MHz) spectrum of **NBF** in $CDCl_3$.

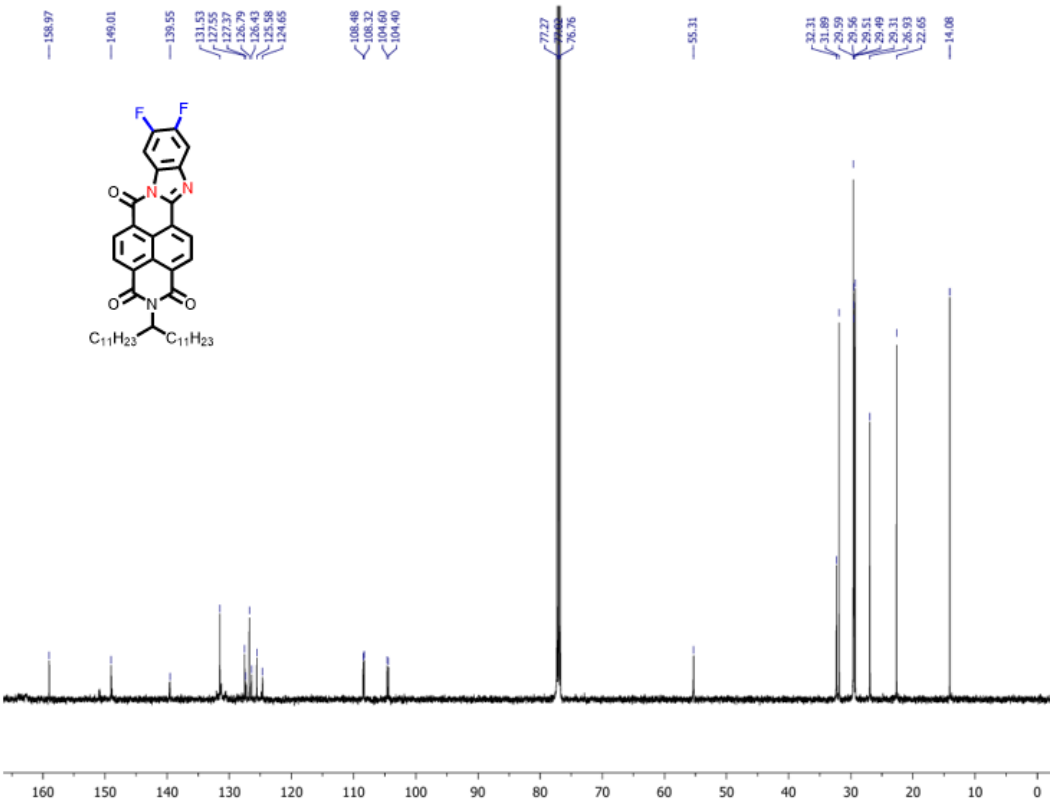


Figure S10. ^{13}C NMR (100 MHz) spectrum of **NBF** in $CDCl_3$.

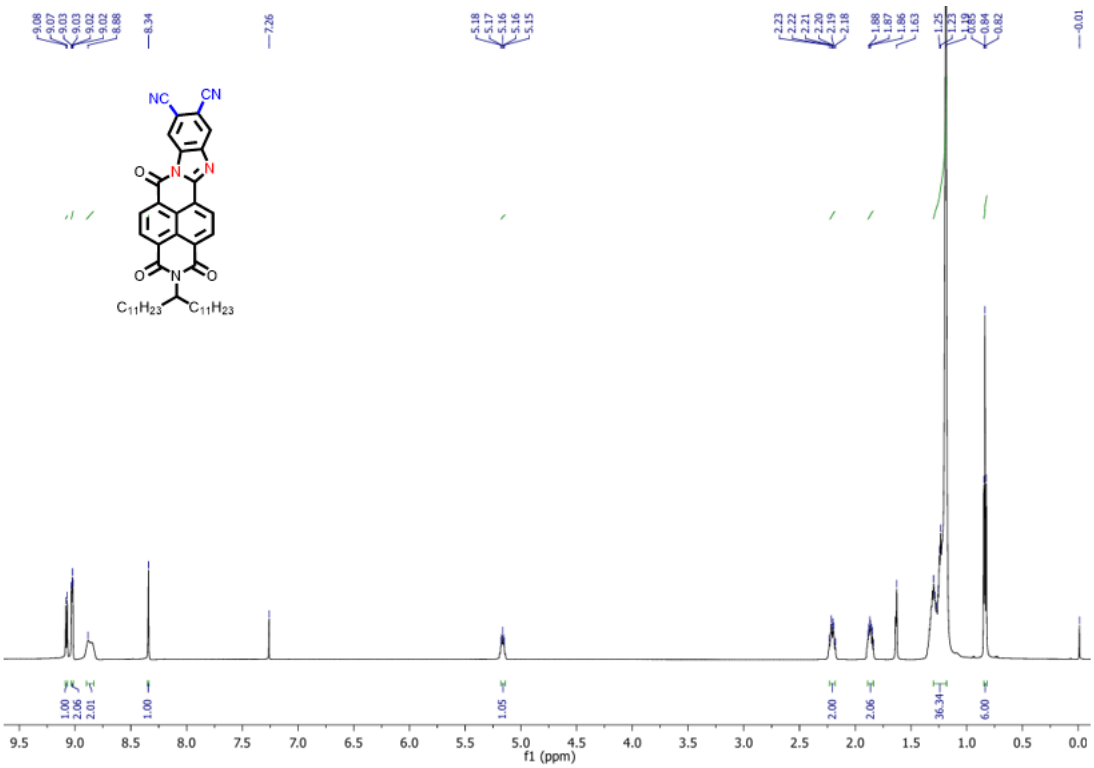


Figure S11. ^{1}H NMR (600 MHz) spectrum of **NBCN** in $CDCl_3$.

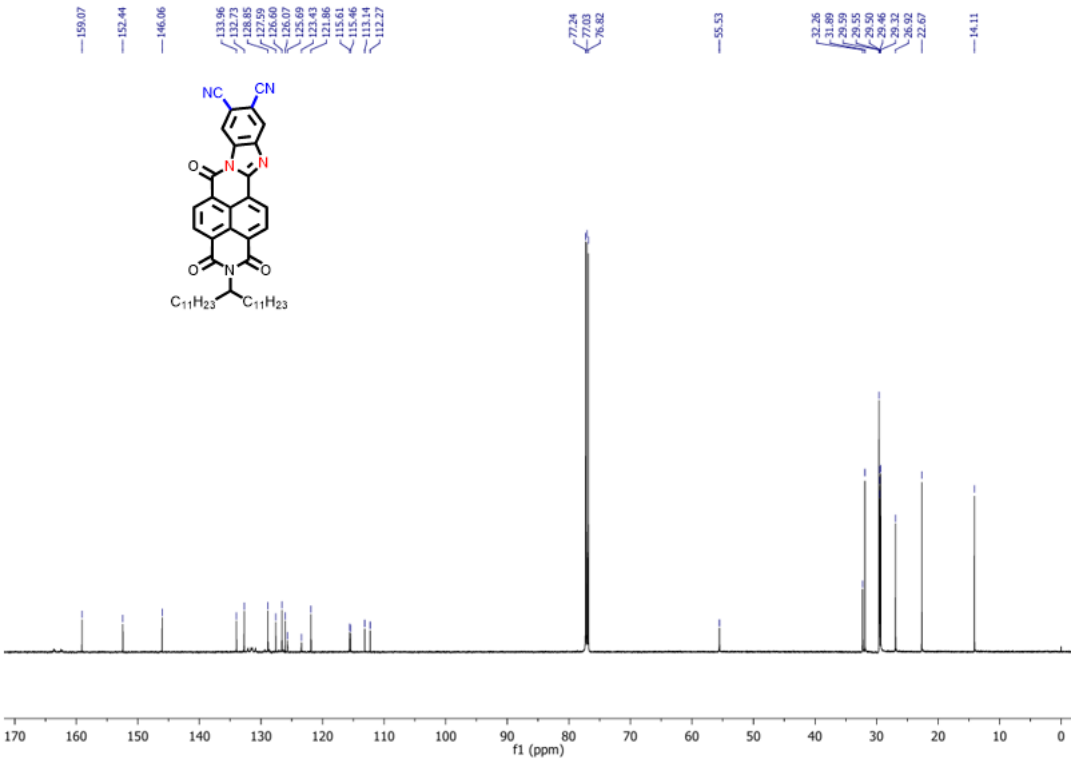


Figure S12. ^{13}C NMR (150 MHz) spectrum of **NBCN** in $CDCl_3$.

4. MALDI-TOF mass spectra

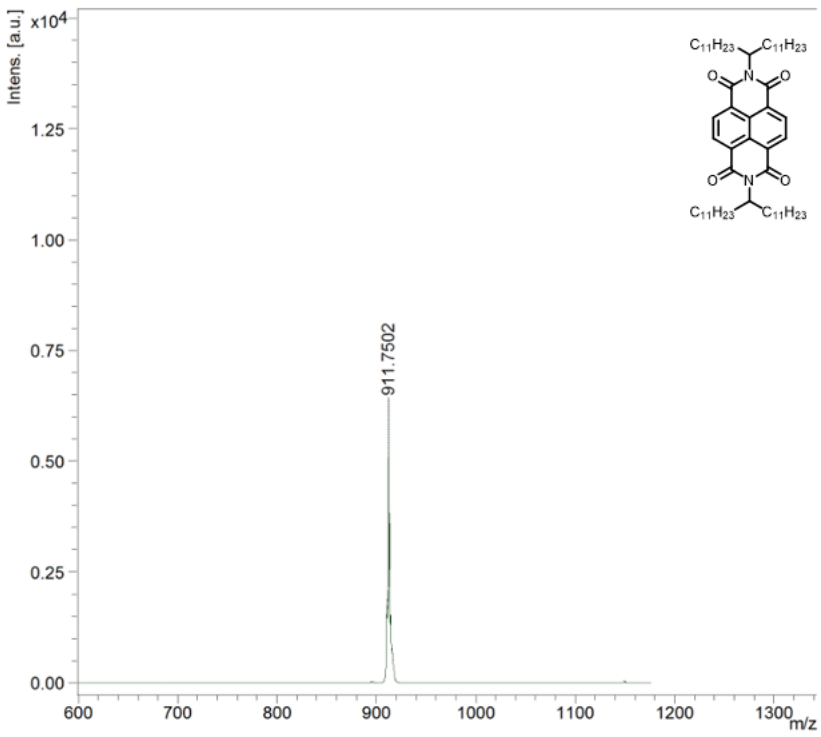


Figure S13. MALDI-TOF mass spectrum of compound **2**.

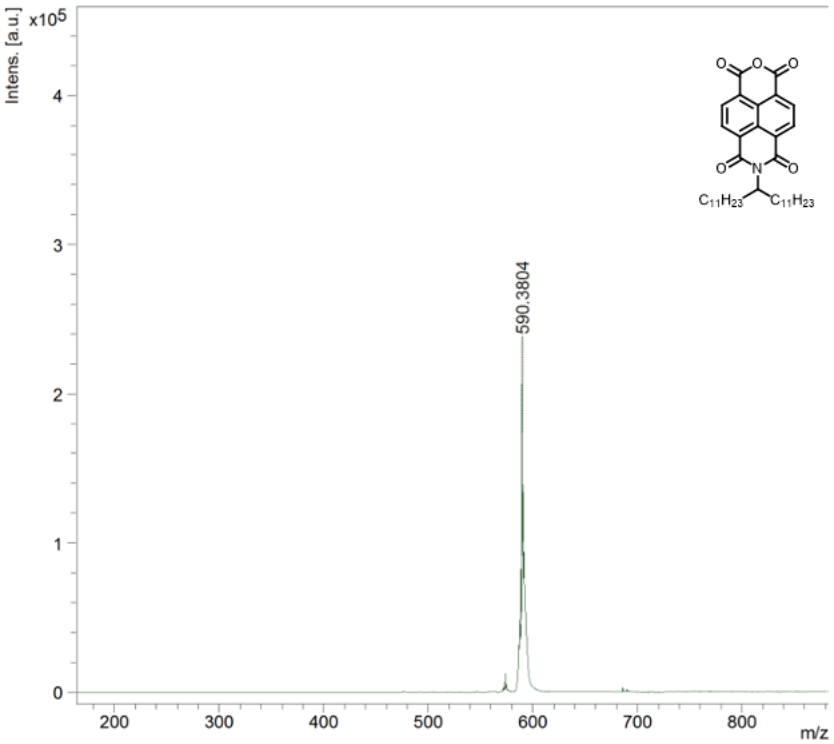


Figure S14. MALDI-TOF mass spectrum of compound **3**.

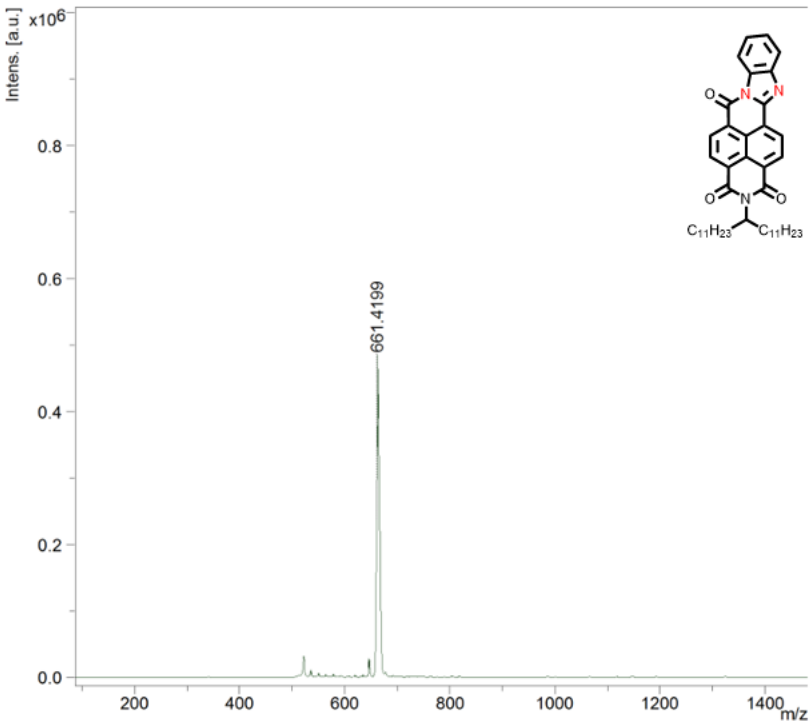


Figure S15. MALDI-TOF mass spectrum of **NB**.

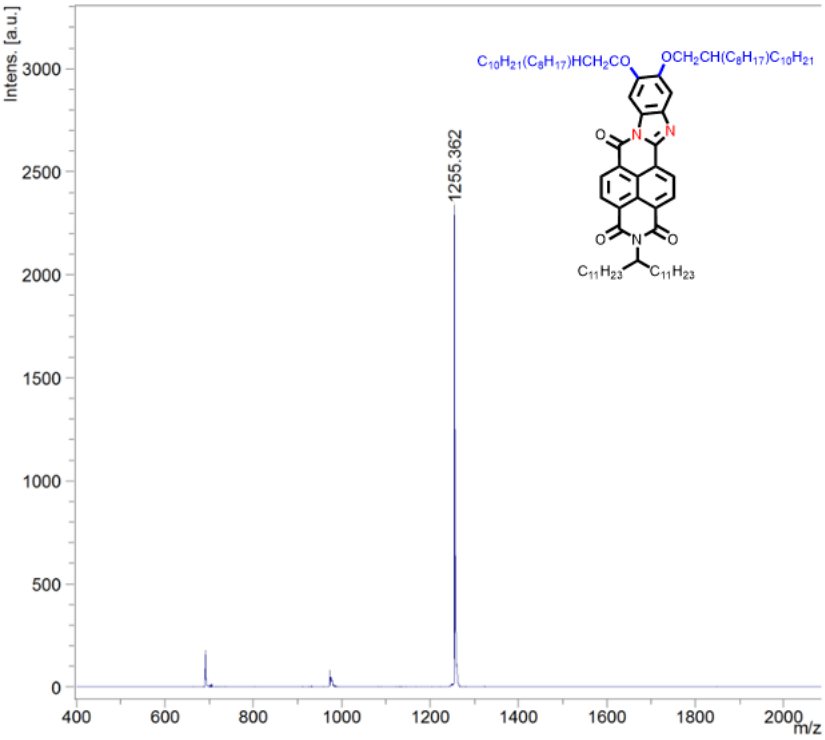


Figure S16. MALDI-TOF mass spectrum of **NB20**.

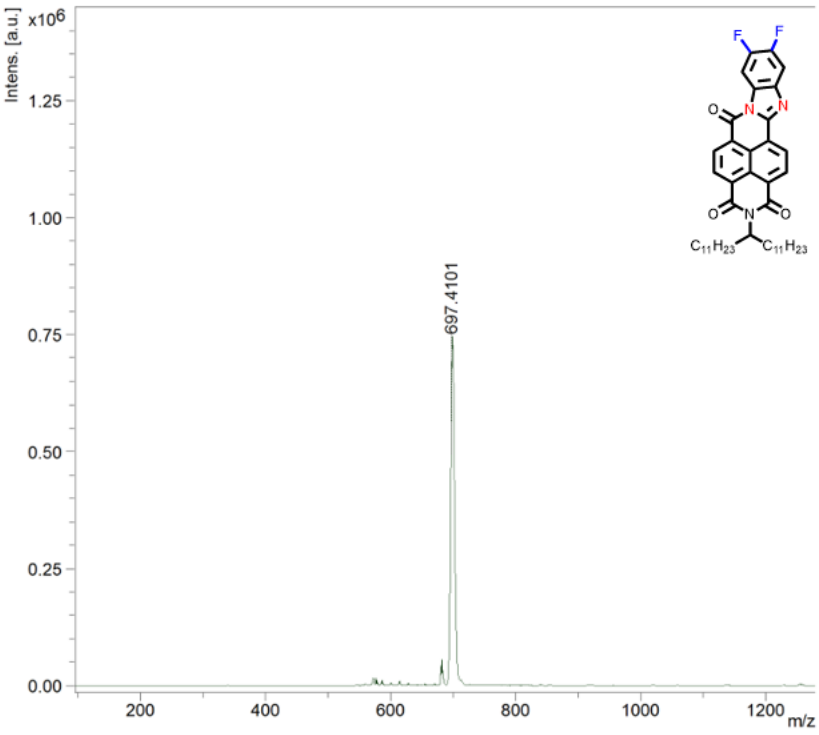


Figure S17. MALDI-TOF mass spectrum of **NBF**.

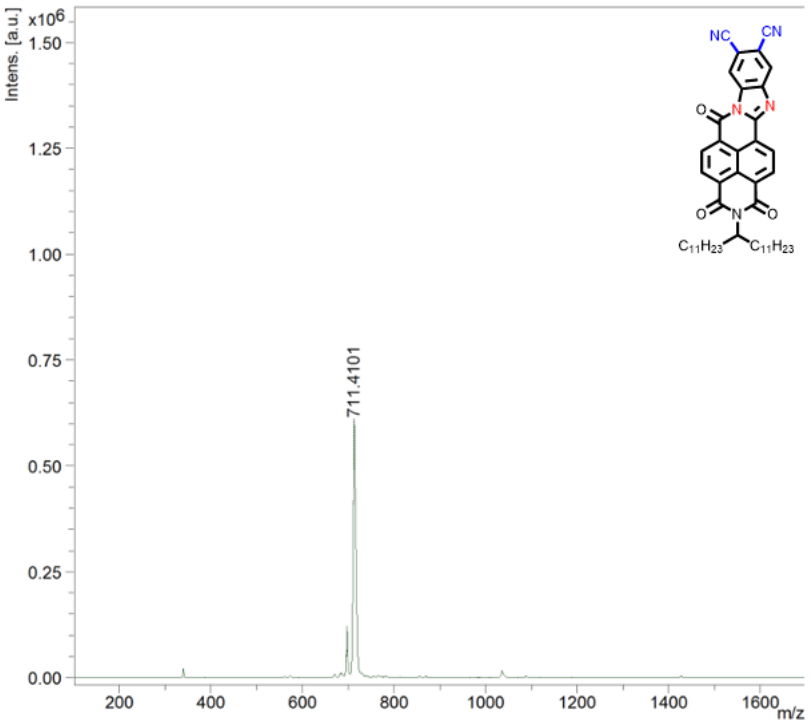


Figure S18. MALDI-TOF mass spectrum of **NBCN**.

5. Polarizing optical microscopy (POM)

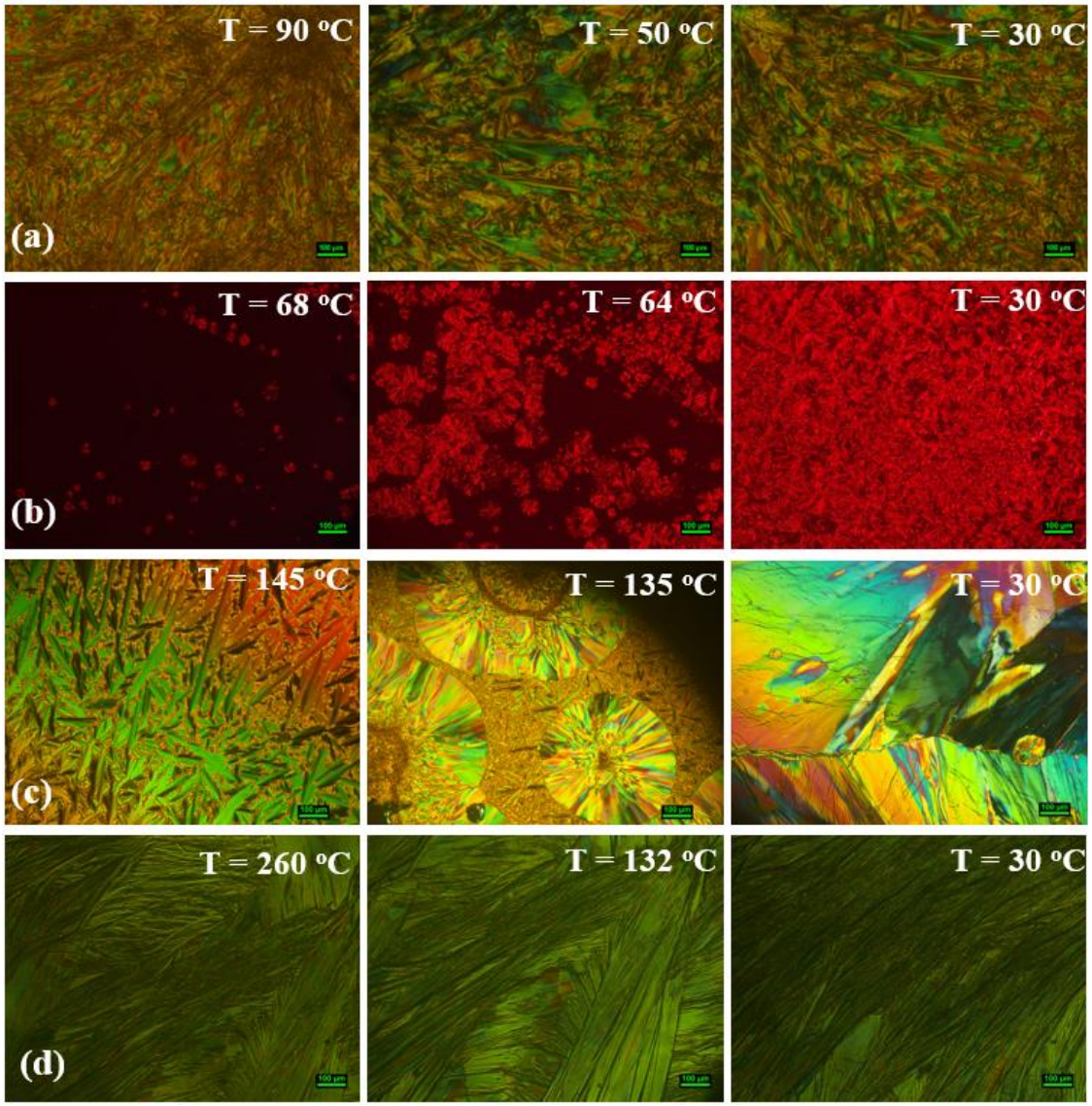


Figure S19. POM images obtained for (a) **NB**, (b) **NB20**, (c) **NBF**, and (d) **NBCN** at different temperatures (scale bar 100 μm).

6. Differential scanning calorimetry (DSC)

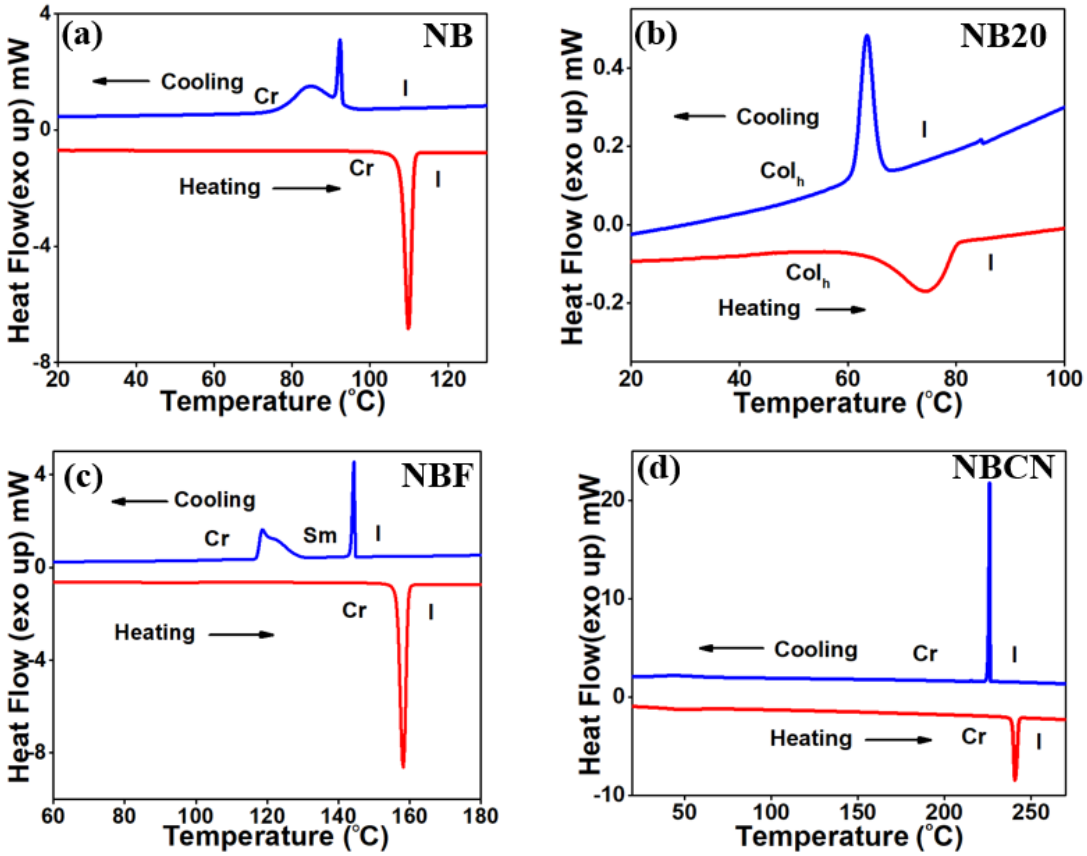


Figure S20. DSC traces for first cooling (blue) and second heating (red) were obtained for (a) **NB**, (b) **NB20**, (c) **NBF**, and (d) **NBCN** at a rate of 5 °C/min.

7. X-ray diffraction studies

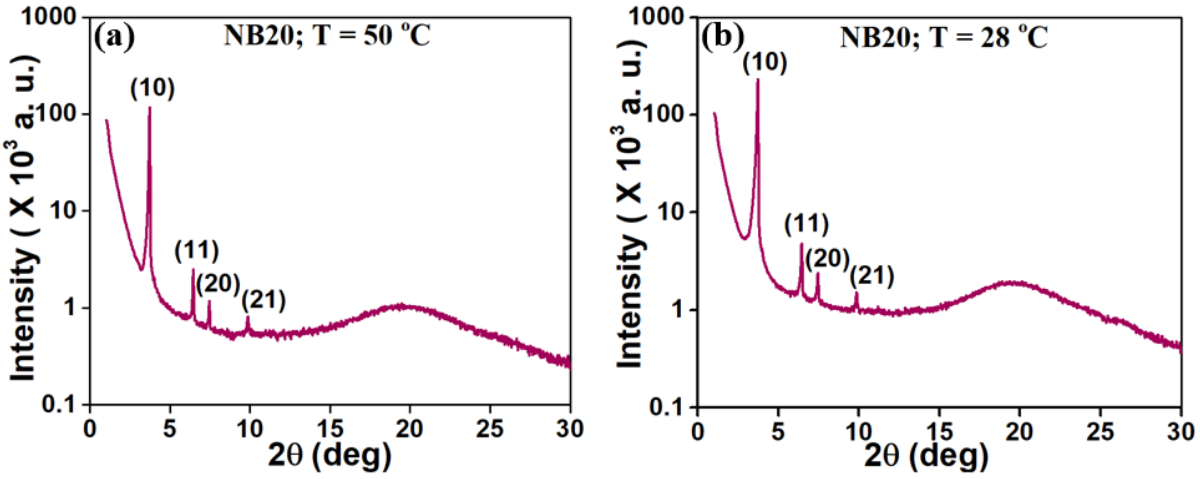


Figure S21. Plot of the intensity against 2θ obtained from the powder XRD pattern of the Col$_h$ phase for compound **NB20** at 50 °C (a) and at 28 °C (b).

Table S1. Results of (hkl) indexation of XRD profiles of the compound **NB20** and **NBF** at a given temperature (T) of mesophases.

Compounds (D/Å)	Phase (T/°C)	d_{obs} (Å)	d_{cal} (Å)	Miller indices *hk*	Lattice parameters (Å), Lattice area S (Å^2), Molecular volume (Å^3)
NB20 (37.02 Å) MW: 1655.01	Col_h (50)	23.66 13.62 11.84 8.96 4.54 (h_a)	23.66 13.66 11.83 8.94	10 11 20 21	a = 27.35 c = 4.54 S = 647.83 V = 2941.16 $Z \approx 1$
	Col_h (28)	23.62 13.68 11.84 8.96 4.56 (h_a) 3.37 (h_c)	23.62 13.63 11.81 8.93	10 11 20 21	a = 27.30 c = 4.56 S = 645.64 V = 2175.80 $Z \approx 1$
NBF (24.42 Å) MW: 697.91	SmA (145)	28.11 4.34 (h_a)			d/L = 1.15
	SmA (135)	27.42 4.46 (h_a)			d/L = 1.12

[a]The diameter (D) of the disk (estimated from Chem 3D Pro 8.0 molecular model software from Cambridge Soft). d_{obs}: spacing observed; d_{cal}: spacing calculated (deduced from the lattice parameters; a for Col_h phase). The spacings marked h_a and h_c correspond to diffuse reflections in the wide-angle region arising from correlations between the alkyl chains and core regions, respectively. Z indicates the number of molecules per columnar slice of thickness h_c, estimated from the lattice area S and the volume V.

8. Photophysical studies

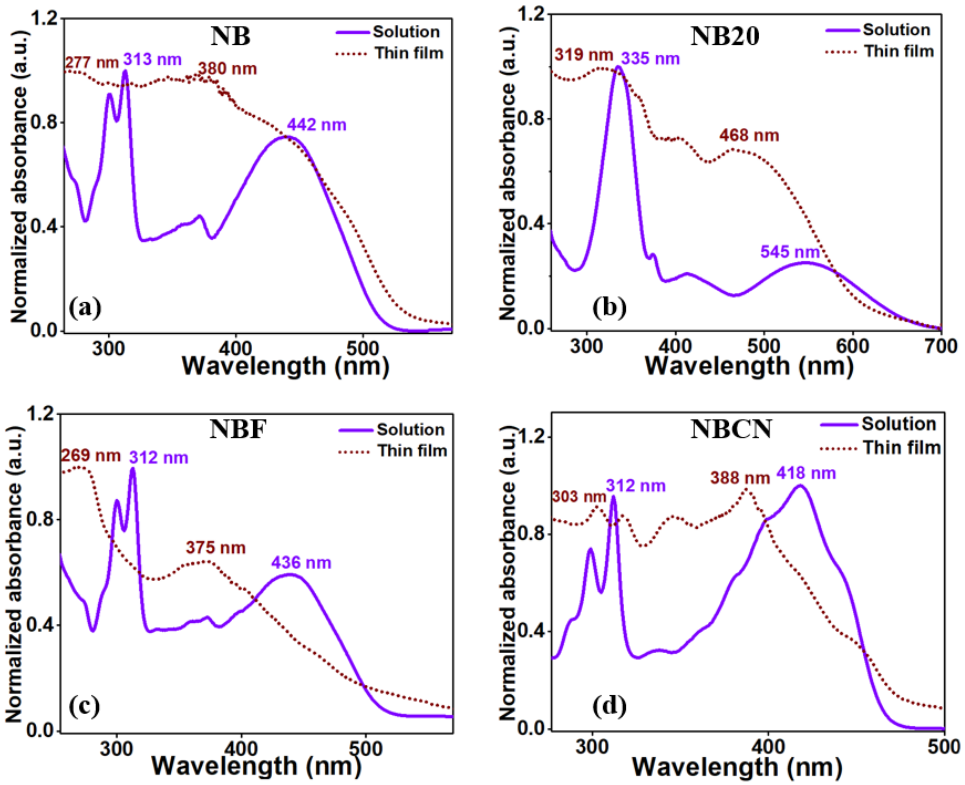


Figure S22. Absorption spectra of compounds (a) **NB**, (b) **NB20**, (c) **NBF**, and (d) **NBCN** in micromolar chloroform solution (solid line) and drop-casted thin films (dotted line).

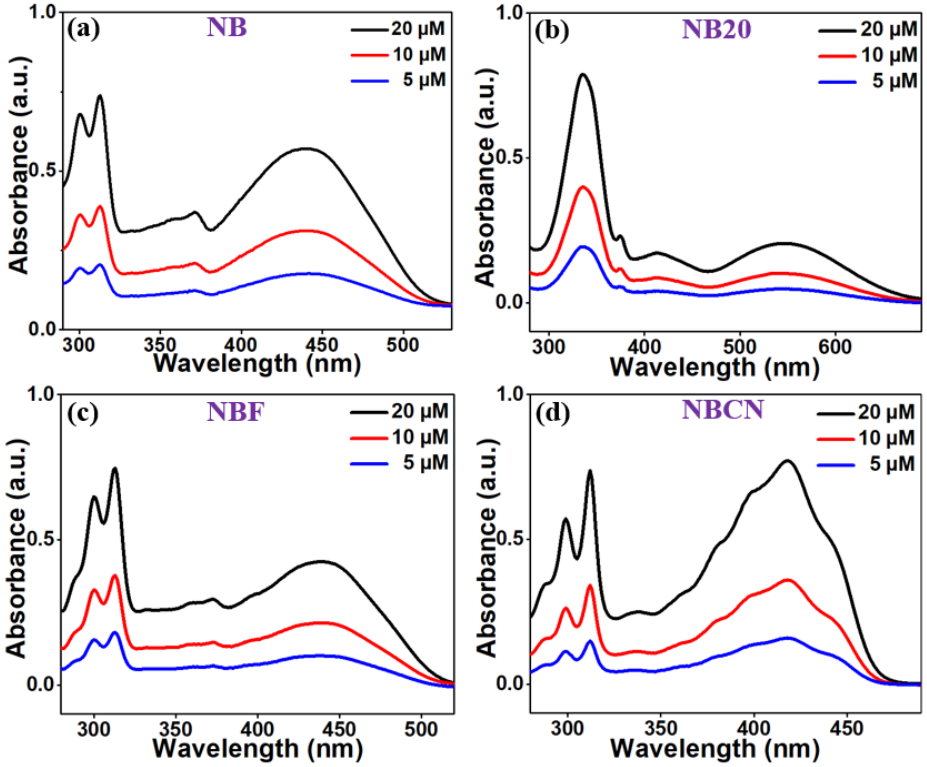


Figure S23. Absorption spectra of compounds (a) **NB**, (b) **NB20**, (c) **NBF**, and (d) **NBCN** in micromolar chloroform solutions as a function of concentration.

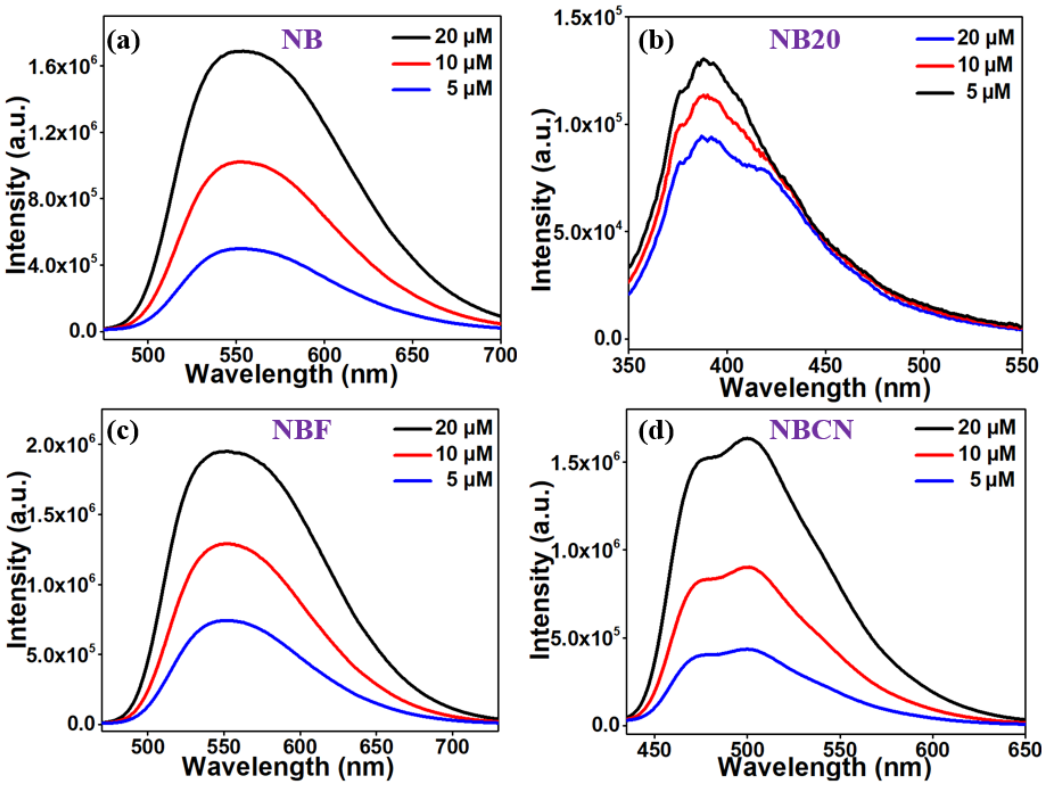


Figure S24. Emission spectra compounds (a) **NB**, (b) **NB20**, (c) **NBF**, and (d) **NBCN** in micromolar chloroform solutions.

9. Time Resolved Photoluminescence Spectroscopy (TRPL)

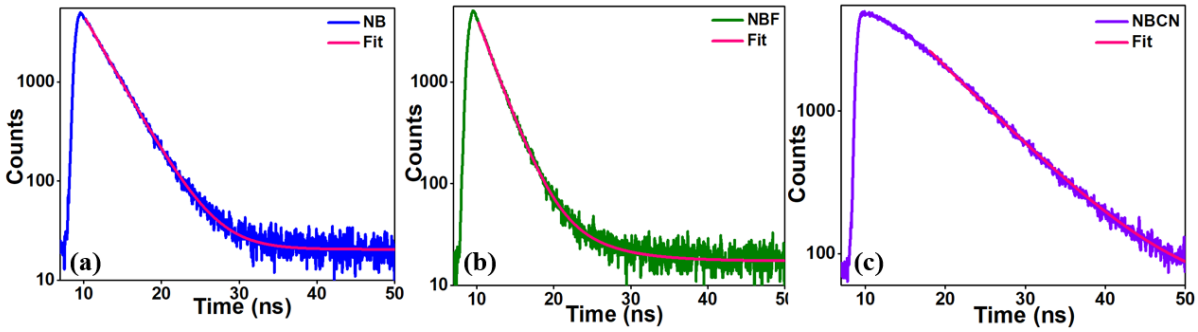


Figure S25. Fluorescence decay curves of (a) **NB**, (b) **NBF**, and (c) **NBCN** in micromolar chloroform solution.

Table S2. Data obtained from time-resolved photoluminescence spectroscopy of **NB**, **NBF** and **NBCN**.[a]

Compound	Average lifetime[b] (τ) (ns)
NB	3.15
NBF	2.40
NBCN	7.72
[a]375 nm laser source used for excitation; [b]20 μM chloroform solution used for experiment.	

10. Electrochemical properties

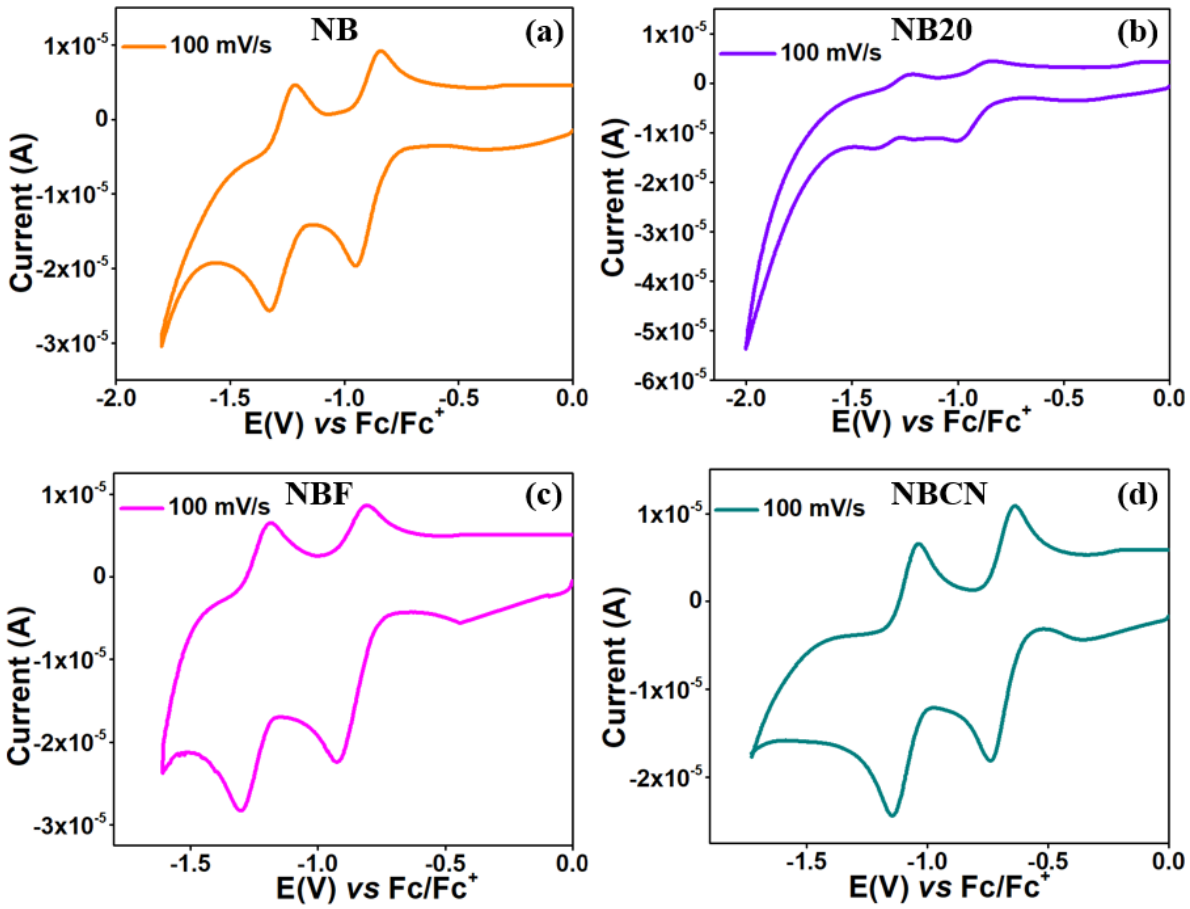


Figure S26. Cyclic voltammogram of compound (a) **NB**, (b) **NB20**, (c) **NBF**, and (d) **NBCN** in 0.5 mM DCM solution.

11. DFT Studies

To understand the electronic properties and frontier molecular orbital energy level of compounds, computational studies were carried out in B3LYP/6-31g(d,p) method using Gaussian 09 program package.[5] The absence of imaginary frequency ensured the energy-minimized structure of all the compounds.

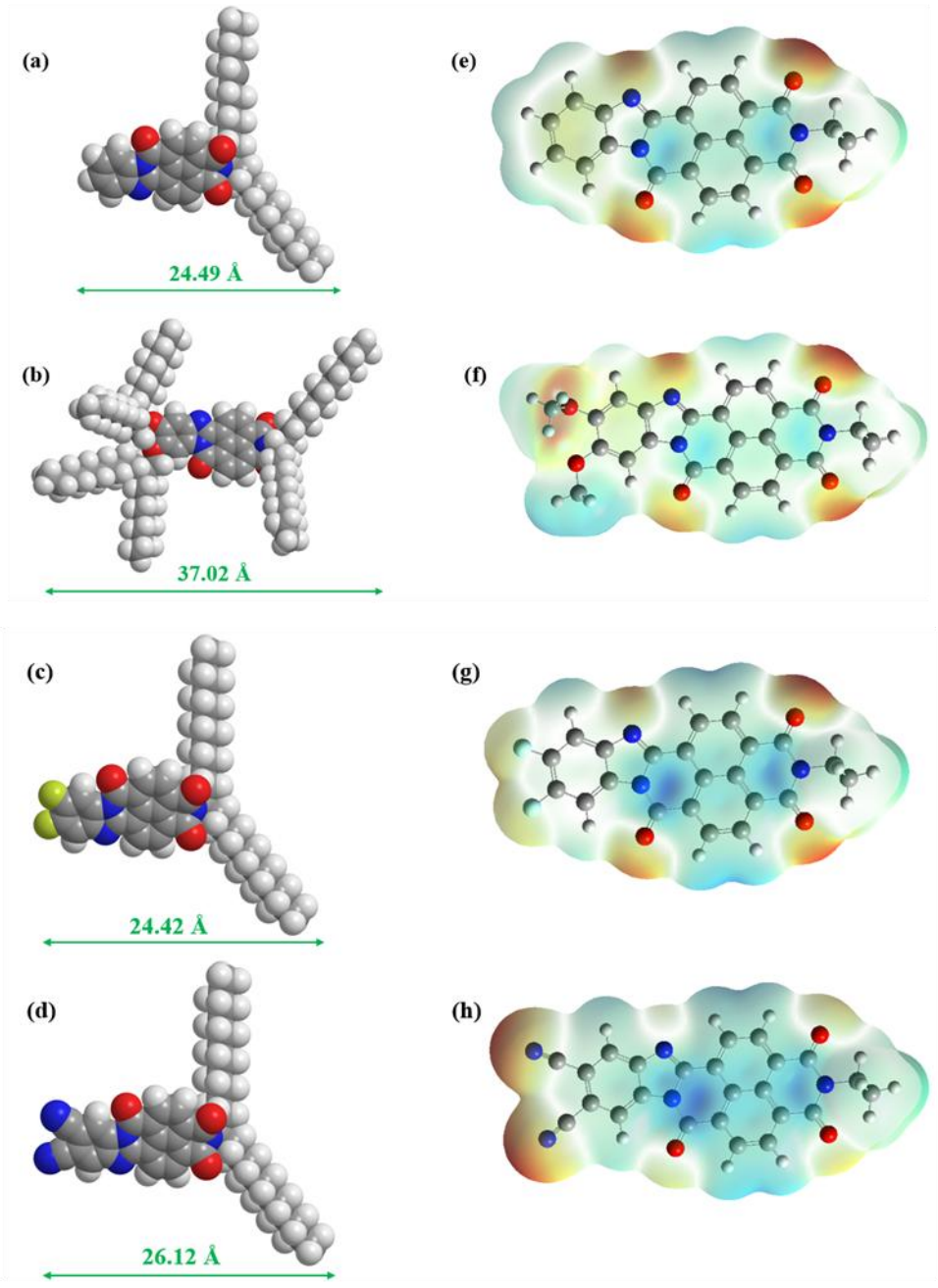


Figure S27. Ground state optimized geometry of (a) **NB**, (b) **NB20**, (c) **NBF**, and (d) **NBCN**; molecular electrostatic potential surfaces of (e) **NB**, (f) **NB20**, (g) **NBF**, and (h) **NBCN** (In the mapped electro-static potential surface, the red and blue colors refer to the electron-rich and electron-poor regions, respectively, whereas the green color signifies the zero electrostatic potential, chain length on the phenyl group is limited to methyl for clarity purpose).

DFT calculation data for NB (chain length limited to isopropyl);

Center No.	Atomic No.	Atomic Type	Coordinates (Angstroms) X	Y	Z
1	6	0	-0.093499	2.541407	-0.000054
2	6	0	-1.492312	2.400834	-0.000098
3	6	0	-2.068697	1.140798	-0.000095
4	6	0	-1.253374	-0.015364	-0.000057
5	6	0	0.161599	0.120311	-0.000037
6	6	0	0.728896	1.424323	-0.000030
7	6	0	-1.837590	-1.303766	-0.000035
8	6	0	-1.027963	-2.430499	-0.000022
9	6	0	0.370843	-2.308050	-0.000015
10	6	0	0.968719	-1.053303	-0.000019
11	6	0	2.407655	-0.878843	-0.000004
12	7	0	2.942961	0.423342	0.000017
13	6	0	2.204610	1.616400	0.000004
14	8	0	2.752445	2.705839	0.000020
15	7	0	3.326592	-1.809171	-0.000004
16	6	0	4.539264	-1.130850	0.000016
17	6	0	4.335206	0.268853	0.000029
18	6	0	5.838237	-1.650509	0.000024
19	6	0	6.896814	-0.747615	0.000046
20	6	0	6.673995	0.642333	0.000060
21	6	0	5.387456	1.181824	0.000053
22	6	0	-3.554037	1.013437	-0.000181
23	7	0	-4.090781	-0.280249	0.000161
24	6	0	-3.314167	-1.459696	-0.000001
25	8	0	-4.270879	2.005655	-0.000469
26	8	0	-3.836951	-2.565611	-0.000063
27	6	0	-5.579411	-0.451323	0.000320
28	6	0	-6.212172	0.102238	1.281918
29	6	0	-6.212295	0.101372	-1.281591
30	1	0	0.367763	3.522939	-0.000042
31	1	0	-2.142375	3.268486	-0.000146
32	1	0	-1.500511	-3.406336	-0.000008
33	1	0	1.004153	-3.188241	-0.000001
34	1	0	5.998118	-2.723252	0.000013
35	1	0	7.916789	-1.119407	0.000053
36	1	0	7.525998	1.315125	0.000078
37	1	0	5.205648	2.248054	0.000063
38	1	0	-5.702485	-1.533786	0.000693
39	1	0	-7.271708	-0.172382	1.302179
40	1	0	-5.738196	-0.331824	2.167736
41	1	0	-6.133920	1.188822	1.334421
42	1	0	-7.271893	-0.173036	-1.301477
43	1	0	-5.738547	-0.333457	-2.167154
44	1	0	-6.133827	1.187905	-1.334913

DFT calculation data for NB20 (chain length limited to isopropyl and methyl);

Center No.	Atomic No.	Atomic Type	Coordinates (Angstroms) X	Y	Z
1	6	0	-1.175260	2.485511	0.053061
2	6	0	-2.576453	2.378514	0.070915
3	6	0	-3.183135	1.132926	0.042120
4	6	0	-2.396794	-0.042284	-0.005546
5	6	0	-0.978893	0.059297	-0.023648
6	6	0	-0.380646	1.349050	0.006567
7	6	0	-3.013204	-1.315363	-0.035152
8	6	0	-2.230332	-2.460738	-0.081982
9	6	0	-0.830000	-2.372999	-0.100295
10	6	0	-0.199322	-1.133397	-0.071704
11	6	0	1.240230	-0.993132	-0.089013
12	6	0	1.098801	1.505961	-0.010922
13	6	0	-4.670899	1.041916	0.061709
14	7	0	-5.239100	-0.237266	0.030630
15	6	0	-4.491418	-1.435563	-0.016683
16	8	0	-5.362916	2.051217	0.103434
17	8	0	-5.043235	-2.527342	-0.041389
18	6	0	-6.730921	-0.372224	0.048162
19	6	0	-7.331435	0.155864	1.355795
20	6	0	-7.368714	0.235729	-1.206028
21	8	0	1.673567	2.582797	0.013394
22	6	0	4.258162	1.010456	-0.077473
23	6	0	3.193232	0.110877	-0.084597
24	6	0	3.365856	-1.287291	-0.130494
25	6	0	4.660356	-1.824466	-0.159699
26	6	0	5.739901	-0.955394	-0.152440
27	6	0	5.542117	0.460671	-0.118508
28	8	0	6.682820	1.202599	-0.139361
29	8	0	7.007327	-1.472818	-0.253050
30	7	0	2.142824	-1.940386	-0.131774
31	7	0	1.807134	0.298219	-0.058224
32	6	0	6.562522	2.619499	-0.151768
33	6	0	7.814678	-1.372975	0.923910
34	1	0	-0.690107	3.455168	0.075113
35	1	0	-3.205519	3.260763	0.107187
36	1	0	-2.726652	-3.424499	-0.104176
37	1	0	-0.219431	-3.268333	-0.137173
38	1	0	-6.880628	-1.450886	0.016753
39	1	0	-8.397282	-0.092612	1.383397
40	1	0	-6.856040	-0.317877	2.220278
41	1	0	-7.224600	1.237937	1.441205
42	1	0	-8.435066	-0.011799	-1.218197
43	1	0	-6.918869	-0.182575	-2.111793
44	1	0	-7.263695	1.321136	-1.226813
45	1	0	4.077363	2.074346	-0.050551
46	1	0	4.831596	-2.893848	-0.198576
47	1	0	7.581877	3.004819	-0.190119
48	1	0	6.008660	2.965471	-1.032608
49	1	0	6.066420	2.989841	0.753722
50	1	0	8.760568	-1.862317	0.684088

51	1	0	8.002233	-0.329915	1.194924
52	1	0	7.342082	-1.893098	1.766967

DFT calculation data for NBF (chain length limited to isopropyl);

Center No.	Atomic No.	Atomic Type	Coordinates (Angstroms) X	Y	Z
1	6	0	-0.678353	2.532682	-0.000481
2	6	0	-2.077572	2.397075	-0.000650
3	6	0	-2.657879	1.138901	-0.000532
4	6	0	-1.846793	-0.020225	-0.000343
5	6	0	-0.431321	0.109810	-0.000268
6	6	0	0.140016	1.412380	-0.000321
7	6	0	-2.436627	-1.306076	-0.000208
8	6	0	-1.632449	-2.436493	-0.000147
9	6	0	-0.233093	-2.320118	-0.000112
10	6	0	0.370311	-1.067918	-0.000153
11	6	0	1.809363	-0.900112	-0.000067
12	6	0	1.614826	1.598984	-0.000202
13	6	0	-4.144416	1.017204	-0.000833
14	7	0	-4.686422	-0.273891	0.001123
15	6	0	-3.914526	-1.455968	-0.000064
16	8	0	-4.856072	2.012833	-0.002597
17	8	0	-4.440369	-2.560155	-0.000638
18	6	0	-6.176307	-0.438870	0.002126
19	6	0	-6.805999	0.119880	1.282880
20	6	0	-6.806888	0.113850	-1.280819
21	8	0	2.172929	2.682767	-0.000206
22	6	0	4.786313	1.160308	0.000102
23	6	0	3.736664	0.243027	0.000043
24	6	0	3.938622	-1.156533	0.000114
25	6	0	5.237164	-1.682604	0.000243
26	6	0	6.282417	-0.777405	0.000300
27	6	0	6.060850	0.613627	0.000231
28	7	0	2.727868	-1.832343	0.000044
29	7	0	2.348204	0.400477	-0.000074
30	9	0	7.134224	1.419838	0.000296
31	9	0	7.555011	-1.209007	0.000425
32	1	0	-0.214113	3.512832	-0.000496
33	1	0	-2.724558	3.266972	-0.000907
34	1	0	-2.109207	-3.410239	-0.000098
35	1	0	0.395717	-3.203544	-0.000026
36	1	0	-6.303855	-1.520775	0.004692
37	1	0	-7.866431	-0.151012	1.304311
38	1	0	-6.333144	-0.313863	2.169430
39	1	0	-6.724249	1.206309	1.333009
40	1	0	-7.867654	-0.155912	-1.299800
41	1	0	-6.335402	-0.324968	-2.165590
42	1	0	-6.723968	1.199941	-1.336514
43	1	0	4.632044	2.230209	0.000048
44	1	0	5.426311	-2.749129	0.000298

DFT calculation data for NBCN (chain length limited to isopropyl);

Center No.	Atomic No.	Atomic Type	Coordinates (Angstroms) X	Y	Z
1	6	0	-1.003825	2.526001	-0.000288
2	6	0	-2.403494	2.394969	-0.000383
3	6	0	-2.987189	1.138524	-0.000324
4	6	0	-2.179713	-0.022875	-0.000213
5	6	0	-0.763847	0.101664	-0.000171
6	6	0	-0.188566	1.402818	-0.000203
7	6	0	-2.774308	-1.306446	-0.000110
8	6	0	-1.977488	-2.441224	-0.000056
9	6	0	-0.577068	-2.330426	-0.000046
10	6	0	0.029776	-1.080405	-0.000094
11	6	0	1.470461	-0.920799	-0.000053
12	7	0	2.014442	0.375653	-0.000054
13	6	0	1.283784	1.583992	-0.000137
14	8	0	1.853795	2.659422	-0.000149
15	7	0	2.383377	-1.860105	-0.000002
16	6	0	3.594533	-1.189643	0.000033
17	6	0	3.399247	0.213154	0.000001
18	6	0	4.886324	-1.717566	0.000097
19	6	0	5.962989	-0.826723	0.000130
20	6	0	5.746474	0.585640	0.000099
21	6	0	4.451290	1.120519	0.000034
22	6	0	-4.475431	1.021640	-0.000514
23	7	0	-5.022470	-0.267164	0.000640
24	6	0	-4.255577	-1.450330	-0.000012
25	8	0	-4.781271	-2.553711	-0.000328
26	8	0	-5.180989	2.020518	-0.001466
27	6	0	-6.514349	-0.426505	0.001258
28	6	0	-7.140885	0.133727	1.282741
29	6	0	-7.141482	0.130061	-1.281534
30	6	0	7.296783	-1.351357	0.000196
31	7	0	8.367392	-1.805116	0.000248
32	6	0	6.860715	1.485283	0.000139
33	7	0	7.748577	2.236529	0.000173
34	1	0	-0.537472	3.505207	-0.000296
35	1	0	-3.047472	3.267031	-0.000529
36	1	0	-2.458982	-3.412518	-0.000005
37	1	0	0.047877	-3.216654	0.000016
38	1	0	5.050287	-2.788383	0.000121
39	1	0	4.283197	2.188460	0.000010
40	1	0	-6.645781	-1.507930	0.002820
41	1	0	-8.202006	-0.133894	1.304036
42	1	0	-6.669577	-0.302099	2.169052
43	1	0	-7.056379	1.219913	1.333584
44	1	0	-8.202783	-0.136956	-1.301324
45	1	0	-6.671002	-0.308793	-2.166786
46	1	0	-7.056342	1.216045	-1.335746

12. OLED device fabrication and measurement:

Electrical and optical measurements were performed in a dark environment at room temperature. Current density, Voltage, and luminance (J–V–L) properties were measured using a CS-100A luminance spectrophotometer (Becker & Hickl, Berlin, Germany) whereas power and current efficiency were determined with a PR-655 spectrophotometer (NLRI, Farum, Denmark). Current & voltage characteristics were measured and analyzed using a Keithley 2400 SMU (Keithley Instruments, Cleveland, OH, USA). The external quantum efficiency (EQE) was calculated with the standard methodology reported in the literature.[6,7]

Preliminary device integration of the NB, NBF, and NBCN emitters in a CBP host matrix confirms its compatibility with solution-processed OLED fabrication and optoelectronic applications. The devices were constructed with the configuration: ITO(125nm)/PEDOT: PSS (35nm)/CBP:x wt.% of NB, NBF, or NBCN (x = 0.5, 2, 5, and 10; 20nm)/TPBi(40nm)/LiF(1nm)/Al (200nm).

OLED devices were fabricated on pre pattern ITO glass substrates, sequentially cleaned with detergent solution for 5 minutes and rinsed with deionized water for up to 10 minutes. The substrates were subsequently ultrasonicated in acetone at 50 °C for 30 min, followed by IPA (Isopropyl alcohol) at 60 °C for a further 30 minutes. After drying, UV treatment was applied for 20 min to eliminate residual contaminants before transferring the substrates into a nitrogen-filled glovebox. Device fabrication was performed inside an inert atmosphere. A PEDOT: PSS (Hole-injection Layer) spin-coating was done at 4000 rpm for up to 20 seconds and annealed at 130 °C for approximate 10 minutes, followed by 10 minutes of cooling. The emissive layer, consisting of NB, NBF, and NBCN in a CBP host, deposited at 2500 rpm by spin-coating for 20 seconds. Subsequently, TPBi, LiF, and an Al cathode were thermally evaporated under high vacuum (~10^{-6} Torr). The active illuminating area of the fabricated OLEDs was 0.09 cm^2.

13. References

1. A. Wicklein, M. A. Muth and M. Thelakkat, *J. Am. Chem. Soc*., 2009, **131**, 14442-14453.
2. P. K. Behera, K. Yadav, N. Kumar, Ravindra Kumar Gupta, D. S. S. Rao, U. K. Pandey and A. S. Achalkumar, *Chem. Commun*., 2023, **59**, 6028–6031.
3. M. J. Tauber, R. F. Kelley, J. M. Giaimo, B. Rybtchinski, M. R. Wasielewski, J. Am. Chem. Soc., 2006, 128, 1782-1783.
4. J. Shao, J. Chang and C. Chi, *Chem. Asian J*. 2014, **9**, 253–260.
5. a) Gaussian 09, Revision B.01, M. J. Frisch, G. W. Trucks, H. B. Schlegel, G. E. Scuseria, M. A. Robb, J. R. Cheeseman, G. Scalmani, V. Barone, B. Mennucci, G. A. Petersson, H. Nakatsuji, M. Caricato, X. Li, H. P. Hratchian, A. F. Izmaylov, J. Bloino, G. Zheng, J. L. Sonnenberg, M. Hada, M. Ehara, K. Toyota, R. Fukuda, J. Hasegawa, M. Ishida, T. Nakajima, Y. Honda, O. Kitao, H. Nakai, T. Vreven, J. J. A. Montgomery, J. E. Peralta, F. Ogliaro, M. Bearpark, J. J. Heyd, E. Brothers, K. N. Kudin, V. N. Staroverov, R. Kobayashi, J. Normand, K. Raghavachari, A. Rendell, J. C. Burant, S. S. Iyengar, J.

Tomasi, M. Cossi, N. Rega, J. M. Millam, M. Klene, J. E. Knox, J. B. Cross, V. Bakken, C. Adamo, J. Jaramillo, R. Gomperts, R. E. Stratmann, O. Yazyev, A. J. Austin, R. Cammi, C. Pomelli, J. W. Ochterski, R. L. Martin, K. Morokuma, V. G. Zakrzewski, G. A. Voth, P. Salvador, J. J. Dannenberg, S. Dapprich, A. D. Daniels, O. Farkas, J. B. Foresman, J. V. Ortiz and J. Cioslowski Fox, D. J. Gaussian Inc., Wallingford, CT, 2009; b) C. Lee, W. Yang and R. G. Parr, Phys. Rev. B, 1988, 37, 785–789; c) A. D. Becke, *J. Chem. Phys*., 1993, **98**, 1372–1377.

6. A. Kumar, S. Lenka, K. Patidar, C. A. Tung, M. Y. Luo, R. Beresneviciute, G. Krucaite, D. Tavgeniene, D. Blazevicius, B. Blazeviciute, J. H. Jou, and S. Grigalevicius, *Molecules*., *Molecules*, 2026, **31**, 1–17.
7. H. Shi, W. Jing, W. Liu, Y. Li, Z. Li, B. Qiao, S. Zhao, Z. Xu, and D. Song, *ACS Omega.,* 2022, **7**, 7893–7900.